Analysis of The Microstrip-Grid Array Antenna and Proposal of A New High-Gain, Low-Complexity, and Planar Long-Range WiFi Antenna

Assimonis, S., Samaras, T., & Fusco, V. (2017). Analysis of The Microstrip-Grid Array Antenna and Proposal of A New High-Gain, Low-Complexity, and Planar Long-Range WiFi Antenna. DOI: 10.1049/iet-map.2017.0548

Published in:
IET Microwaves, Antennas and Propagation

Document Version:
Peer reviewed version

Queen's University Belfast - Research Portal:
Link to publication record in Queen's University Belfast Research Portal

IET Microwaves, Antennas & Propagation

Submission Template for IET Microwaves, Antennas & Propagation

IET Journals
The Institution of Engineering and Technology

ISSN 1751-8644
doi: 0000000000
www.ietdl.org

Analysis of The Microstrip-Grid Array Antenna and Proposal of A New High-Gain, Low-Complexity, and Planar Long-Range WiFi Antenna

Stylianos D. Assimonis[1] ✉, *Theodoros Samaras*[2], *Vincent Fusco*[1]

[1] *School of Electronics, Electrical Engineering and Computer Science, Queen's University Belfast, Belfast BT3 9DT, United Kingdom*
[2] *School of Physics, Aristotle University of Thessaloniki, Thessaloniki 54124, Greece*
✉ *E-mail: s.assimonis@qub.ac.uk*

Abstract:
This work presents a systematic numerical analysis of the microstrip-grid antenna aiming not only to explore the antenna performance limits in terms of frequency impedance bandwidth and maximum gain, but also to use this analysis as a starting point for further optimization. The obtained antenna has dimensions $297\ \mathrm{mm} \times 210\ \mathrm{mm} \times 9.9\ \mathrm{mm}$ and at 2.41 GHz, has a maximum gain of 15.4 dB, which is very close to the directivity of an ideal, lossless aperture antenna with the same dimensions, at the same frequency. Measurements have shown that the antenna operates from 2.38 to 2.51 GHz (i.e., across the WiFi-band with a 5.32% frequency bandwidth relative to $50\ \Omega$), with maximum radiation efficiency 98.2%, while the latter remains over than 91% for the whole WiFi-band, and finally has a measured half-power beamwidth of 18.5 and 34.5 deg. in the horizontal and vertical planes, respectively. Thus,the antenna is suitable candidate for long-range WiFi links.

1 Introduction

Five decades have passed since the wire-grid antenna was proposed by J. D. Kraus [1]. The latter is a high-gain, linearly polarized, backward angle-fire travelling-wave antenna, which consisted of a grid, adjacent to a rectangular ground plane in order to enhance its gain. The grid is a periodic structure of rectangular frames with dimensions equal to about one wavelength by one-half wavelength. The radiation originates from the short edges, while long edges act as transmission line feed elements. The distance between wire-grid and ground-plane affects mostly the frequency impedance bandwidth (i.e., reflection coefficient magnitude less than -10 dB), which is usually narrow, and the radiation pattern: for a distance less than one-quarter wavelength (e.g., about 0.1λ), radiation takes place mainly due to the fringing fields at the short edges of the frames and gain is maximized. When the distance is exactly one-quarter wavelength, the ground plane acts as a reflector, decreasing the gain and increasing the frequency impedance bandwidth. Moreover, increasing the number of short edges increases the gain and also the size of the antenna.

In [2] a microstrip-grid antenna was proposed. This was a variant of the wire-grid antenna: actually the wires were replaced by microstrip lines with changing widths, in order to control the microstrip line impedance and finally the amplitudes of the first sidelobes.

Since 1994, H. Nakano and his associates have published several works [3–12] related to the wire-grid antenna. Most of these [3–7], focus on far-field characteristics. In [3] the wire-grid antenna was modified in order to radiate broadside to the grid. Here the authors changed the feeding point and showed that the short and long edges should be equal to 0.54λ and 1.08λ, respectively, while the distance of ground plane should be less than 0.2λ. In [4–7] the antenna was modified to radiate either a dual linear or a circularly polarized wave. n [8–10] authors reported on the applied numerical method, which was used to analyze wire-grid arrays, while in [11] they attempted to minimize the antenna dimensions by adopting a meander instead of straight-shape wires: the antenna-size reduction was in the order of 38% and the antenna gain also reduced about 2 dB.

The wire-grid, in its original form, has an input impedance greater than $50\ \Omega$ [6, 8, 10, 11] and a narrow frequency impedance bandwidth: in [6] and [11] the authors achieved a 1.5% and 2.6% VSWR bandwidth (BW) relative to $55\ \Omega$ and $160\ \Omega$, respectively. Hence, it is an engineering challenge how not only to increase frequency impedance bandwidth, but also how to reduce input impedance close to $50\ \Omega$, without affecting the radiation pattern.

Towards this direction, authors in [12, 13] modified the wire-grid antenna: the rectangular frames of the grid had long and short sides of different microstrip line width. After optimization, in [12] the antenna had a simulated VSWR bandwidth of approximately 13% and maximum simulated directivity of about 18 dB at 7 GHz. However, the authors did not mention relative to which impedance this bandwidth was achieved. In [13] the obtained VSWR bandwidth was 4.5% relative to $50\ \Omega$, while the maximum measured gain was 18.3 dB at 2.45 GHz. It is noted, that in both cases [12, 13] the short edges number was 13, while in our work the analysed/proposed antenna has 7 short edges elements (the number of short edges increases the maximum achieved gain, as mentioned).

In [14] a novel wire-grid antenna was proposed. Short and long edges of rectangular frames were replaced by elliptical radiation elements and sinusoid transmission lines, respectively. The main idea is that, elliptical elements lead to enhanced frequency impedance bandwidth, while sinusoid transmission lines reduce the total antenna size. The grid lies on a substrate, which is at a distance from the ground plane. Feeding takes place via a coaxial cable. After optimization with genetic algorithms (GA) in conjunction with the finite difference in time domain (FDTD) method, the proposed antenna had a frequency impedance bandwidth of 25% and maximum gain 13.7 dB at about 2.45 GHz. However, it is noted that optimization procedure took 110 hours in a cluster system, while it would need more than 1000 hours without parallel computation. In [15] short edges were also replaced by elliptical elements and a linearly tapered ground plane was used. Optimization took place on a cluster system (32 processors), also, and after 112 hours the proposed antenna achieved frequency impedance bandwidth 25.6% and maximum antenna gain 15.1 dB at 5.8 GHz. Consequently, according to [14, 15], it is evident that the use of elliptical shaped short

Table 1 Microstrip-Grid Antenna Matched to 50 Ω Comparisons

	Freq. (GHz)	BW (%)	Gain (dB)	Ratio (%)	RE (%)	Rad. Elem.	Resources/ Comp. Time
[13]	2.45	4.5	18.3*	–	–	13	200 iterations
[14]	2.4	25	13.7*	66	–	7	cluster 32 processors 110 hours
[15]	5.8	25.6	15.1**	56	–	7	cluster 32 processors 112 hours
this work	2.41	5.32	15.4*	69	98.2	7	laptop (4-cores) 12 MB RAM 0.5 hour 6 iterations

*simulation, **measurement.

edges increases the antenna frequency impedance bandwidth, but also demands very high computational resources. An overview at microstrip-grid antennas matched to 50 Ω is given in Table 1: our proposed antenna operates in the whole WiFi-band, has the maximum gain and designed after a low demanding design procedure in terms of computational resources and time, compared to prior-art designs. Table 1 presents the ratio of the maximum achieved gain of each antenna to the maximum directivity of an ideal, lossless antenna with the same dimensions and at the same frequency, based on the maximum effective aperture [18], as will be explained in next section.

The main contribution of this work is a) to perform a systematic investigation, which points not only how to estimate the performance limitation of the microstrip-grid antenna in terms of impedance bandwidth and gain, but also how to substantially reduce the design procedure time/computational resources in future designs, b) to propose a simple/low-complexity, light-weight, easy fabricated antenna, which has high radiation efficiency (RE), is pure linear polarized and has narrow beamwidth, which in turn leads to high-received and low-interference power, and thus to propose a candidate antenna for long-range WiFi links.

Actually, the proposed antenna has been successfully deployed in a wireless sensor network (WSN), which manages the drinking water reservoirs in urban areas, specifically in the island Crete (Greece), where the link-range was extended to 5 km using the antenna developed in this paper.

2 Antenna Design

In this section the microstrip-grid antenna, in its initial form (Fig. 1), will be numerically analyzed in order to examine the influence of dimension parameters on the frequency impedance bandwidth relative to 50 Ω and on the maximum gain at 2.45 GHz. It is noted that the antenna size was fixed at 297 mm × 210 mm, i.e., the size of an A4 paper sheet, aiming to keep the antenna as compact as possible, but also to maximize the antenna gain, as will explained in next section. Next the antenna will be modified, aiming at performance enhancement in terms of frequency impedance bandwidth.

2.1 Microstrip-Grid Antenna Analysis

A typical microstrip-grid antenna geometry is depicted in Fig. 1. The antenna consists of a microstrip line grid, which is closely adjacent to a rectangular ground plane, at distance h. Microstrip lines have constant width, w. Rectangular frames have a size of $l \times s$, while the whole antenna geometry has $a \times b$ size (i.e., 297 mm × 210 mm in our case). Feeding takes place via an SMA connector. Between the grid and the ground plane there is only air.

In order to investigate the influence of dimensions l, s and w on frequency impedance bandwidth and maximum gain at point

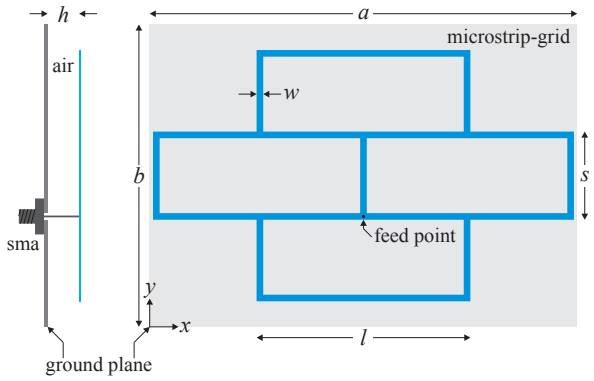

Fig. 1: A typical microstrip-grid antenna geometry.

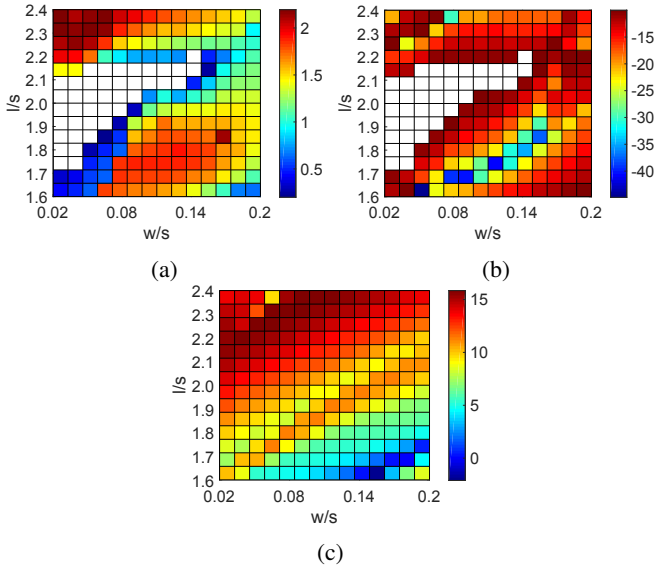

Fig. 2: Antenna analysis simulated results versus design parameters l and w
a Frequency impedance bandwidth relative to 50 Ω
b Reflection coefficient magnitude in dB with reference impedance of 50 ohm
c Maximum simulated gain at $(\phi, \theta) = (0, 0)$ and frequency 2.45 GHz

$(\phi, \theta) = (0, 0)$ and frequency 2.45 GHz, the antenna was analysed via Ansys HFSS (ANSYS Inc., Canonsburg, PA, USA) with the Integral Equation (IE) method. When s and h were fixed at 0.5λ (λ is wavelength at frequency of 2.45 GHz) and 0.08λ, respectively, while l and w varied from $1.6s$ to $2.4s$ and from $0.02s$ to $0.2s$, respectively. Fig. 2a depicts the simulated frequency impedance bandwidth relative to 50 Ω within the WiFi band, i.e., from 2.4 to 2.5 GHz. The latter was estimated through the reflection coefficient parameter, S_{11}, with reference impedance at 50 ohm. In turn, the frequency impedance bandwidth relative to 50 ohm is, $\text{BW} = (f_{\max} - f_{\min})/f_{\text{centre}}$, where, the $f_{\max}$ and $f_{\min}$ is the higher and lower frequency of the frequency bandwidth in which $|S_{11}|$ is less than -10 dB, and f_{centre} is the mean value of $f_{\max}$ and $f_{\min}$. In each parameter set, if there is more than one resonance frequency (i.e., $|S_{11}| < -10$ dB), the resonance with the higher BW is chosen. On the other hand, if there is no resonance (i.e., $|S_{11}| > -10$ dB) the BW is set to zero (white/blank colour in Fig. 2a). Thus, the optimization goal was the maximization of the BW when the antennas is resonating.

It is evident that the bandwidth is maximized when the ratio l/s is around 2.3 and w/s less than 0.08. More specifically, maximum bandwidth (2.19%) took place for $l/s = 2.3429$ and $w/s = 0.0714$. Hence, despite the fact that the optimum set of parameters lies close to the upper and lower limit of the l and w parameter, respectively,

it is not close enough to that limits in order to extend them and test more l, w variations. Additionally, these limits are not arbitrary: since the antenna ground plane has fixed size of 297 mm $\times$ 210 mm (i.e., the size of an A4 paper sheet), and in order to keep the size of the antenna wire-grid less than the ground plane size, and given the fact that the wire-grid has dimensions $(2l - w) \times (3s - 2w)$, it turns out that for the lowest ratio of $w/s = 0.02$ the l/s ratio is no more than 2.437. For all the above reasons, the l/s and w/s ratio is no more than 2.4 and no less than 0.02, respectively, during the sweep parameter analysis. The white/blank colour denotes the parameters set in which the antenna does not operate.

In Fig. 2b, the corresponding reflection coefficient magnitude, with reference impedance of 50 ohm is depicted alongside with the frequency impedance bandwidth (Fig. 2a). It is noted that the maximum illustrated magnitude is less than -10 dB, while for higher values, where the antenna does not operate, the reflection coefficient magnitude does not depicted (white/blank area).

Fig. 2c depicts the maximum simulated gain at $(\phi, \theta) = (0, 0)$ and frequency 2.45 GHz for respective l and w variations. It is observed that maximum gain (15.85 dB) occurs for $l/s = 2.3429$ and $w/s = 0.0971$. Hence, in order to simultaneously maximize the frequency bandwidth and the gain, the microstrip-grid antenna should have l/s around 2.3429 and w/s equal to about 0.08. However, the bandwidth remains narrow. In order to overcome this problem, a modified antenna is next presented.

2.2 *Modified Microstrip-Grid Antenna Analysis*

The proposed antenna is illustrated in Fig. 3. The only difference between the original form (Fig. 1) and the modified antenna is the adoption of a resistor, R, which electrically connects the microstrip-grid and the ground at a specific point. The main idea is that the resistor placement reduces the antenna input impedance and thus the frequency impedance bandwidth is expanded [16]. The possible problem with this solution is that the resistor increases ohmic losses, which compromises antenna efficiency. According to prior art (e.g., [16]) the maximum gain reduction is about 2 dB.

In order to examine the influence of resistor placement on frequency impedance bandwidth and maximum gain at point $(\phi, \theta) = (0, 0)$ and frequency 2.45 GHz, the antenna was analysed again via Ansys HFSS and the Integral Equation (IE) method. The dimensions s and h were fixed again at 0.5λ and 0.08λ, respectively, while now $l/s = 2.3429$ and $w/s = 0.0843$ (i.e., the average of 0.0714 and 0.0971 according to the previous analysis). The dimension g and resistance R varies from $-0.4s$ to $0.4s$ and from 0.1 to 50 Ω, respectively. The simulated frequency impedance bandwidth relative to 50 Ω is depicted in Fig. 4a. It is observed that the bandwidth is maximized when the ratio g/s is greater than 0.25 and R varies from about 4 to 30 Ω; the maximum bandwidth (i.e., 2.98%) was achieved for $g/s = 0.2857$ and $R = 17.9214$. On the other hand, for $g/s < -0.22$ (i.e., the resistor is placed close to feeding point) the antenna does not resonate.

In Fig. 4b, the corresponding reflection coefficient magnitude, with reference impedance of 50 ohm is depicted alongside with the frequency impedance bandwidth (Fig. 4a). It is noted that the maximum illustrated magnitude is less than -10 dB, while the white/blank area denotes that the antenna does not resonate (i.e., magnitude higher than -10 dB).

The maximum simulated gain and RE in front of the antenna (i.e., $(\phi, \theta) = (0, 0)$) at 2.45 GHz for respective g and R variations is depicted in Fig. 4c and 4d, respectively. Now, maximum gain (15.85 dB) occurs for $g/s = 0.1714$ and low resistance $R = 0.1$. We note that, even for maximum resistance $R = 50\ \Omega$, when $0 < g/s < 0.2$ maximum gain remains higher than 15.5 dB (Fig. 4c), while the radiation efficiency is always above 96.5%. Hence, resistor adoption does not significantly affect antenna performance in terms of gain (as will be also explained in next Section). In conclusion, when aiming at both maximum frequency impedance bandwidth and gain, the microstrip-grid antenna should have $g/s > 0.2$ and $4 < R < 30\ \Omega$.

However, according to the above parametric numerical analysis, the antenna in the optimal case ($g/s = 0.2857$ and $R = 17.9214$)

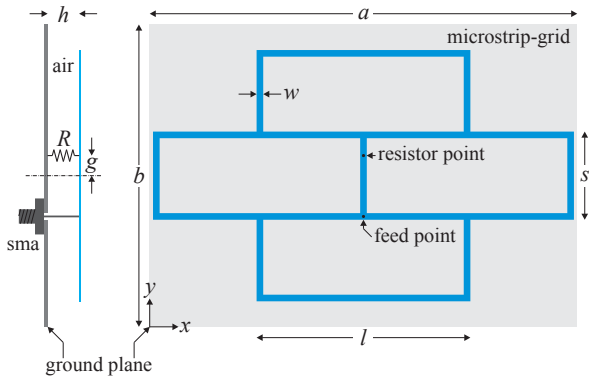

Fig. 3: The proposed, modified microstrip-grid antenna geometry.

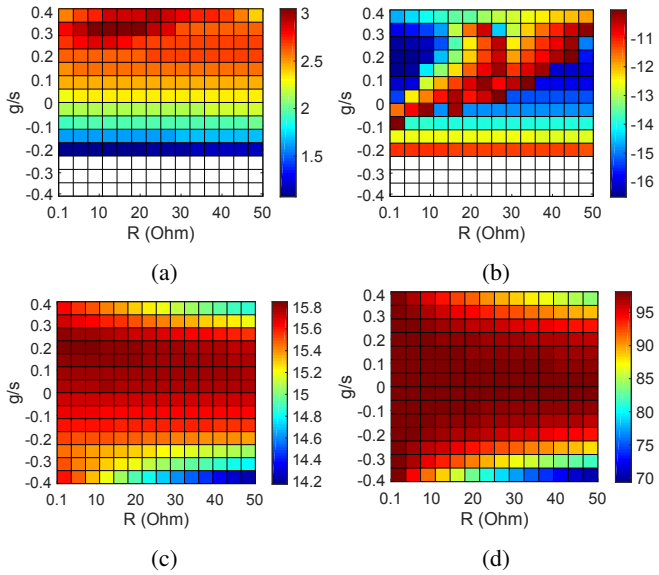

Fig. 4: Antenna analysis simulated results versus design parameters g and R
a Frequency impedance bandwidth relative to 50 Ω
b Reflection coefficient magnitude in dB with reference impedance of 50 ohm
c Maximum simulated gain at $(\phi, \theta) = (0, 0)$ and frequency 2.45 GHz
b Maximum simulated RE at $(\phi, \theta) = (0, 0)$ and frequency 2.45 GHz

has frequency impedance bandwidth 2.98% and maximum gain 15.5 dB at $(\phi, \theta) = (0, 0)$ and 2.45 GHz. In the next section, the modified microstrip-grid antenna will be optimized in order to further expand the frequency bandwidth aiming an operation from 2.4 to 2.5 GHz, i.e., in the whole WiFi frequency range.

3 Modified Microstrip-Grid Optimization

In this section, the initially modified microstrip-grid antenna dimensions will be predicted using light optimization, in terms of computational resources, in order to increase frequency impedance bandwidth and ensure acceptable performance from 2.4 to 2.5 GHz. Next, it will be fabricated and measured in terms of reflection coefficient and antenna realized gain.

3.1 *Optimization*

The Quasi-Newton algorithm was applied in conjunction with the IE method and Ansys HFSS. For excitation, a coaxial transmission line with wave port was applied. The area between microstrip-grid and ground plane was filled with substrate ($\epsilon_r = 1.04$, $\tan\delta = 0.0001$), while all metallic parts were considered as copper sheet with zero thickness and finite conductivity of 5.8×10^7 S/m. The

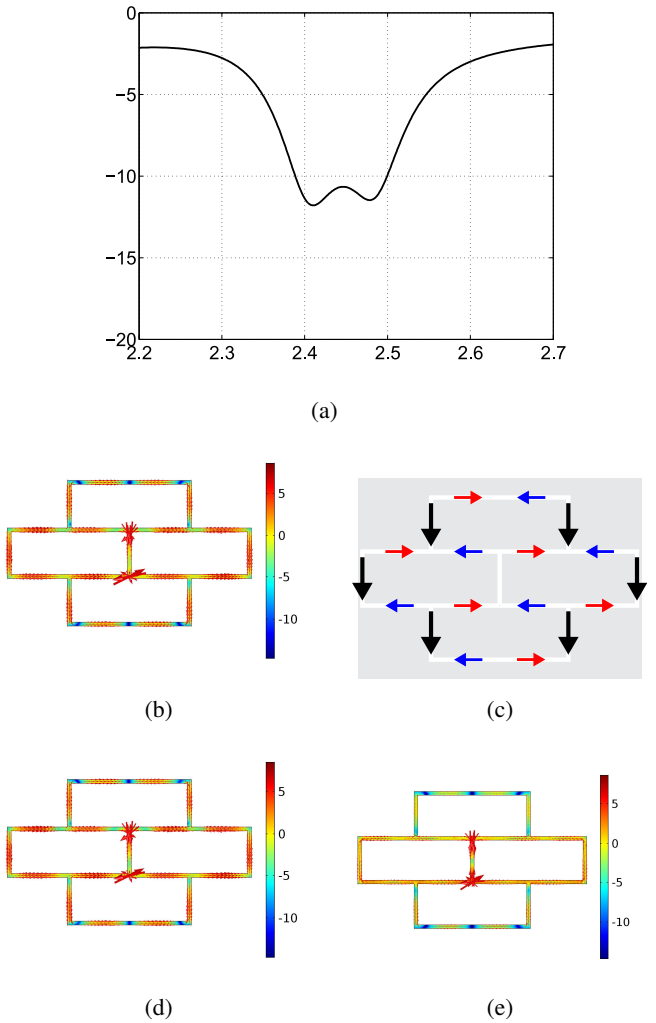

Fig. 5: Simulated and measured reflection coefficient of the proposed antenna (a), the surface current distribution (in dB) at 2.45 GHz (magnitude and vectors) along the microstrip-grid (b) and the schematic representation of the vectors (c): the currents in the horizontal edges (i.e., in parallel to x-axis - red/blue vectors) are mutually exclusive in terms of far-field because they have opposite direction, while the currents in the vertical edges (i.e., in parallel to y-axis - black vectors) are added in phase and result the radiation pattern. It is also depicted the surface current distribution for the first (d) and second (e) minima of the simulated reflection coefficient, and specifically at 2.41 and 2.485 GHz respectively.

latter emerged as a result of the fabrication process and will be explained below. Dimensions l, s, w, g and resistance R were the degrees of freedom, while h was fixed at 9.9 mm (0.0809λ). Antenna size was again fixed at $a \times b = 297$ mm $\times$ 210 mm. All design parameters can take continuous values except R, which can take only discrete values. The fitness function was the reflection coefficient magnitude to be less than -10 dB for $2.4 - 2.5$ GHz and the maximization of the antenna gain. Moreover, $s = 0.5\lambda$, $l/s = 2.3429$, $w/s = 0.0843$, $g/s = 0.2857$ and $R = 18$ were used as initial point for the optimization, according to the previous parametric analysis. The problem converges after 6 iteration and about 30 minutes (on a 4 cores laptop with 12 MB RAM) and the optimal design parameters values were: $l = 148.49$ mm, $s = 61.25$ mm, $w = 4.6$ mm, $g = 22.51$ mm and $R = 18\ \Omega$.

Fig. 5a depicts the simulated reflection coefficient relative to 50 Ω: the antenna operates in the frequency band $2.39 - 2.5$ GHz, namely operates in the whole WiFi frequency band and has 4.5% simulated frequency impedance bandwidth. The surface current distribution in the microtrip-grid at 2.45 GHz is depicted in Fig. 5b: the

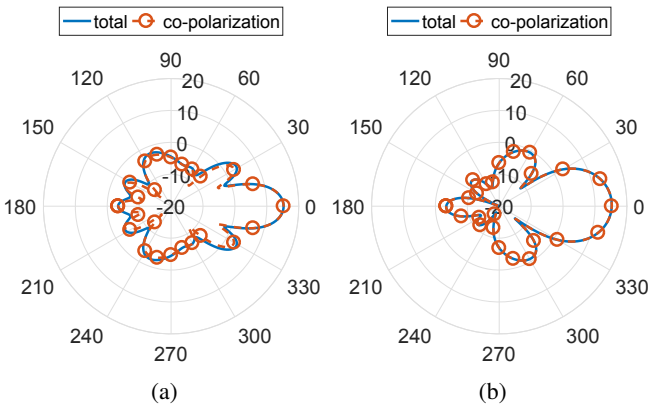

Fig. 6: Total and co-polarized, simulated antenna gain at 2.45 GHz: antenna presents high gain, narrow HPBW and is highly linear polarized
a In the zx-plane.
b In the zy-plane.

currents is mainly concentrated in the six radiation elements, i.e., the vertical edges, which are in parallel to y-axis, while the horizontal edges (i.e., those in parallel to x-axis) act as transmission lines, as expected [1]. Specifically, the schematic representation of the vectors is depicted in Fig. 5c. Again, it is observed that the currents in the horizontal edges (i.e., red/blue vectors) are mutually exclusive in terms of far-field because they have opposite direction, while the currents in the vertical edges (i.e., black vectors) are added in phase and finally results the radiation pattern. Equivalently, the microstrip-grid acts as an antenna array with six, in our case, dipole-like radiating elements, which are adjoining with a ground plane.

From the reflection coefficient diagram in Fig. 5a it is observed that there are two minima, the first at 2.41 and the second at 2.485 GHz, respectively. In order to explain the dual-resonant shape of the curve, the surface current distribution was estimated via simulation and is also depicted in Fig. 5d and 5e. It is observed that in the both cases the radiation mechanism is the same and also the same with the case of 2.45 GHz (Fig. 5b and 5c): antenna radiates mainly through the short edges, while the long edges are acting as waveguides. However, for the case of the 2.485 GHz, the current distribution of the central short edges is slightly sifted to the corner of the edges, resulting current misalignment with the other short edges and length reduction of the current path. The latter leads to the shift of the resonance frequency to higher frequencies (i.e., 2.485 GHz). Additionally, the current distribution in the upper short edges is reduced compared with the current distribution of the other short edges, resulting again current misalignment. Finally, it is obvious that the current distribution is much higher in the load, rather in the short radiating elements. Thus, the latter in combination with the aforementioned current misalignment, results to the reduction of the RE at this frequency, as will explained below.

Next, antenna was simulated in terms of radiation pattern: the simulated antenna total gain in dB for 2.45 GHz is depicted in Fig. 6. In the zx-plane the half power beamwidth (HPBW) is 18.7 deg., while in the zy-plane is 31 deg. Antenna appears to have narrow beamwidth, which leads to high-received and low-interference power in a WiFi link. The co-polarized antenna gain (in dB) is a also depicted: in the both planes the antenna is highly linear polarized especially from -12 to 12 deg., in other words when gain is greater than 10 dB.

Fig. 7a depicts the simulated antenna gain and the RE versus frequency: it is observed that over the whole WiFi band the antenna presents high gain, i.e., over than 14 dB and high RE, i.e., greater than 91%. In particular, gain is greater than 15.3 dB until 2.45 GHz, dropping to 14 dB at 2.5 GHz. This happens because as the wavelength decreases, the electrical distance between the ground plane and the microstrip-grid is changing, and it is known that gain is sensitive to the height of the grid [3] and it is maximized in a specific frequency/wavelength [3–6, 8, 11, 12, 14, 15]. Additionally, the

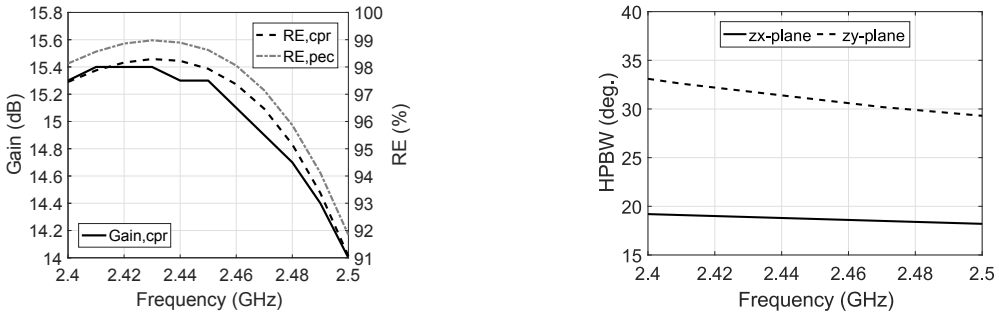

(a) (b)

Fig. 7: Antenna radiation pattern simulation analysis versus frequency at 2.45 GHz.
a Maximum simulated gain and RE for metallic parts considering as copper (cpr) and perfect electric conductor (pec).
b HPBW in the zx- and zy- plane respectively.

antenna radiates mainly due to the fringing fields at the vertical edges of the grid cells, which are maximized at a specific antenna height for a given frequency/wavelength. The 1.4 dB gain variation, in the whole WiFi frequency is lower than the acceptable threshold of 3 dB in a typical communication link.

Moreover, the effect of finite conductivity in the antenna RE is also presented in Fig. 7a: the antenna's RE was again simulated but now using perfect electric conductor (pec) for the metallic parts. It is evident that the RE with finite conductivity is lower compared with pec-case, however the difference is maximum 1%, and thus marginal.

Finally, in Fig. 7b the HPBW versus frequency is depicted in both the horizontal and vertical plane: HPBW varies from 19.2 to 18.2 deg. and from 33.1 to 29.3 deg. in the horizontal and vertical plane, respectively, and thus, the antenna presents almost constant narrow beamwidth in the both planes.

3.2 Electrical size and Maximum Directivity

According to Harrington [17], the maximum directivity, D_0, of a lossless antenna, which completely fills a sphere with radius R is given by,

$$D_0 = (kR)^2 + 2kR \tag{1}$$

where k is the wavenumber.

Additionally, assuming that the proposed microstrip-grid array is an aperture antenna, the maximum directivity is given by,

$$D_0 = \frac{4\pi}{\lambda^2} A_{\mathrm{em}} \tag{2}$$

where λ is the wavelength and A_{em} is the *maximum effective aperture* [18], which it is assumed in this case that is equal to the physical area of the proposed antenna. Hence, at 2.4 GHz the new antenna presents gain 4.7 and 1.7 dB less than the maximum, ideal directivity according to (1) and (2), respectively. It is noted that the ideal estimated directivity in the both cases does not take into account any losses (e.g., in any metallic or dielectric antenna's part), as well as the RE of the antenna. The above considerations are depicted in Fig. 8, which illustrates the maximum ideal directivity based on (1) and (2) and the simulated antenna gain. Moreover, the proposed antenna, which is planar, poorly utilizes the available volume within the sphere of radius R, with attendant decrease in the maximum achieved directivity [18]. Thus, despite the fact that the comparison with (2) is more appropriate, for the shake of completeness, the comparison with the (1) is also included, as it refers to the general case of any antenna shape, planar or not.

Finally, it is noted that the antenna ground dimensions (i.e., a and b in Fig. 3) affect the antenna directivity, as confirmed experimentally: usually, greater size leads to higher gain/directivity. However, in this work it was attempted not only to keep the antenna as compact as possible, but also to reach the maximum ideal directivity given the antenna size based on (2).

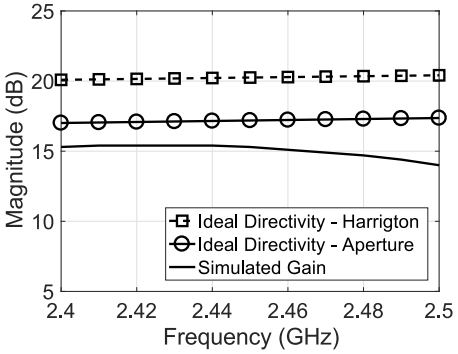

Fig. 8: Simulated gain in dB of the proposed antenna. Also depicted is the maximum directivity of an ideal antenna with the same dimensions based on Harrington's work [17] and on maximum effective aperture [18].

Table 1 presents the ratio of the maximum achieved gain of each antenna to the maximum directivity of an ideal, lossless antenna with the same dimensions and at the same frequency, based on the maximum effective aperture [18]. Specifically, in [13] the total antenna size is not provided, and thus the aforementioned ratio could not be estimated. In [14], it is referred that a margin of 10 mm surrounds the antenna wire-grid, and hence the estimated antenna size is 175.5 mm $\times$ 250.4 mm. In [15], the antenna has size of 126 mm $\times$ 100 mm, while in our case the antenna size is 294 mm $\times$ 210 mm. Additionally, the maximum gain is 13.7 dB at 2.4 GHz, 15.1 dB at 5.8 GHz and 15.4 dB at 2.41 GHz in [14], [15] and in our case, respectively, and thus, the ratio is estimated at 66%, 56% and 69%, respectively, as tabulated in Table 1.

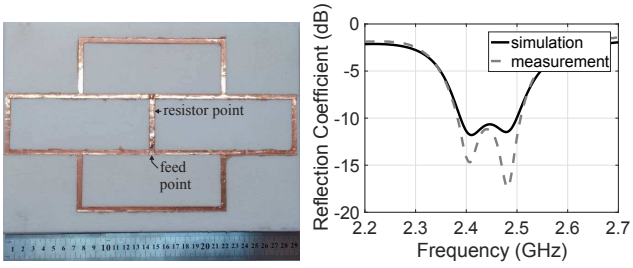

(a) (b)

Fig. 9: The fabricated antenna (a) and the antenna reflection coefficient relative to 50 Ω (b).

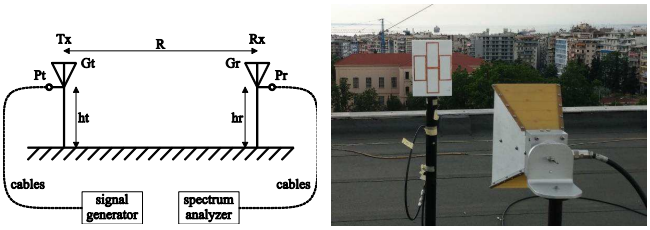

(a) (b)

Fig. 10: The three antennas measurement method [18] topology for the estimation of the realized gain of an antenna (a) and a snapshot of the measurement (b).

3.3 Fabrication and Measurement

Next, the copper antenna pattern was fabricated via the low-cost and low-complexity vinyl-cutting technique, which is a relative low-cost and low-complexity fabrication technique. Low-cost, foam material with $\epsilon_r = 1.04$ and $\tan\delta = 0.0001$ was used to fill the area between the ground plane and the microstrip-grid. Feeding took place through an SMA connector, while the resistor was embedded into the substrate. The fabricated antenna is illustrated in Fig. 9a.

The fabricated antenna was measured in terms of reflection coefficient and realized gain. The measurements shown that the antenna operates from 2.38 to 2.51 GHz (Fig. 9b) resulting a 5.32% frequency impedance bandwidth.

The antenna realized gain was measured with the method of three antennas, as described in [18], with measurement topology presented in the below Fig. 10. The antennas are placed in distance R and all the three possible combinations were tested, using each time one antenna as transmitter and the other as receiver. Thus, using the Friss equation for free space is,

$$G_{\mathrm{r},i} + G_{\mathrm{t},i} = 20\log_{10}\left(\frac{4\pi R}{\lambda}\right) + P_{\mathrm{r},i} - P_{\mathrm{t},i} \qquad (3)$$

where $G_{\mathrm{r},i}$, $G_{\mathrm{t},i}$ is the realized gain (in dB) of the transmitter and the receiver antenna, respectively, $P_{\mathrm{t},i}$ the input power (in dBm) in the transmitter and $P_{\mathrm{r},i}$ the output power (in dBm) in the receiver, and finally $i = a, b, c$ and $j = b, c, a$, indicate the three antennas. It is noted that realized gain (i.e., $((1 - |S_{11}|^2) \times$ gain)), takes into account the return loss because of the mismatch between the signal generator, the spectrum analyser and the antennas. Moreover, the cables losses should be taken into account in the measurement and in our case were about 1 dBm in each cable. The a antenna was the *EM-6952 Electro-Metrics Log-Periodic Antenna* with gain provided by the manufacturer 5.7 dB at 2.45 GHz and the b antenna was the *3115 Double-Ridged Guide Antenna* with gain provided by the manufacturer 9.3 dB at 2.5 GHz. After measurement at 2.45 GHz in the zx- and zy- plane, the maximum realized gain of the proposed wire-grid antenna was 14.8 dB (with measured reflection coefficient of -11.44 dB at the same frequency), which is very closed to the simulated realized gain of 14.93 dB at 2.45 GHz, resulting a good agreement between simulations and measurements. The simulated and measured antenna realized gain in the both zx- and zy- plane is depicted in Fig. 11, where a good agreement is observed again. Additionally, the estimated through measurement antenna half-power beamwidth is 18.5 and 34.5 deg. in the zx- and zy- plane, respectively.

4 Conclusion

In this work, a systematic numerical study of the microstrip-grid antenna was conducted. Performance limits in terms of frequency impedance bandwidth and maximum gain were examined. Next, the antenna was modified based on these findings. The proposed antenna then requires only light-touch optimization when fabricated and measured. Very good agreement between measurements and simulations was observed.

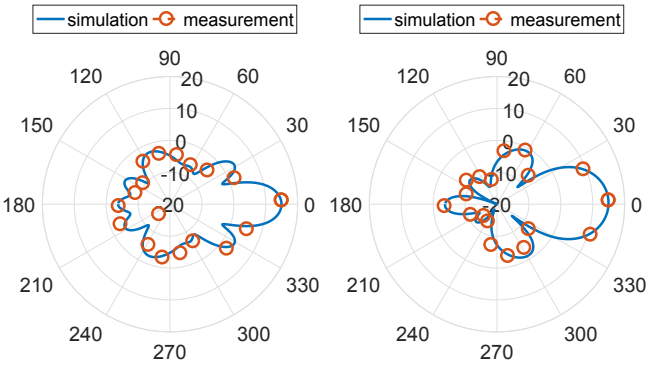

(a) (b)

Fig. 11: Simulated and measured antenna realized gain in dB at 2.45 GHz in the zx- (a) and zy- (b) plane.

The antenna resonates across the whole WiFi frequency band, is high-gain, low-cost, low-complexity, has high radiation efficiency and narrow beamwidth. Consequently, it is a perfect candidate for outdoor, high-distance WiFi links, indeed.

It has already been used for the deployment of a wireless sensor network in Crete, where it is used, which manages drinking water reservoirs in urban areas, where it extended WiFi link-range over to 5 km.

5 Acknowledgments

The authors would like to thank G. Voutsis, V. Papadakis and P. Oikonomakos for their help in various steps throughout this work. This work was supported by the SYN11-6-925 AquaNet project, which was executed within the framework of the "Cooperation 2011" program of the Greek General Secretariat for Research & Technology (GSRT), funded through European Union and Greek National Funds.

6 References

1 Kraus, J. D.: 'A backward angle-fire array antenna', *IEEE Trans. Antennas Propag.*, 1964, **12**, (1), pp. 48–50

2 Conti, R., Toth, J., Dowling, T., Weiss, J.: 'The wire grid microstrip antenna', *IEEE Trans. Antennas Propag.*, 1981, **29**, (1), pp. 157–166

3 Nakano, H., Oshima, I., Mimaki, H., Hirose, K., Yamauchi, J.: 'Center-fed grid array antennas'. Proc. EEE Antennas Propag. Soc. Int. Symp, Newport Beach CA, USA, June 1995, **4**, pp. 2010–2013

4 Kawano, T., Nakano, H.: 'Cross-mesh array antennas for dual LP and CP waves'. Proc. IEEE Antennas Propag. Soc. Int. Symp., Orlando, FL, USA, July 1999, **4**, pp. 2748–2751

5 Nakano, H., Kawano, T., Yamauchi, J.: 'A cross-mesh array antenna'. Proc. 11th lnt. Conf. Antennas Propag., Manchester, UK, April 2001, pp. 327–330

6 Kawano, T., Nakano, H.: 'A grid array antenna with C-figured elements', *Electron. Commun. Japan (Part I: Commun.)*, 2002, **85**, (1), pp. 58–68,

7 Nakano, H., Osada, H., Mimaki, H., Iitsuka, Y., Yamauchi, J.: 'A modified grid array antenna radiating a circularly polarized wave'. Proc. IEEE Int. Symp.

Microw. Antenna Propag. EMC Technol. Wireless Commun., Hangzhou, August 2007 pp. 527–530
8 Nakano, H., Oshima, I., Mimaki, H., Yamauchi, J., Hirose, K.: 'Numerical analysis of a grid array antenna'. Proc. Int. Conf. Commun. Syst., Singapore, November 1994, **2**, pp. 700–704
9 Nakano, H., Kawano, T., Mimaki, H., Yamauchi, J.: 'Analysis of a printed grid array antenna by a fast MoM calculation technique'. Proc. 11th lnt. Conf. Antennas Propag., Manchester, UK, April 2001, pp. 302–305
10 Nakano, H., Kawano, T., Kozono, Y., Yamauchi, J.:, 'A fast MoM calculation technique using sinusoidal basis and testing functions for a wire on a dielectric substrate and its application to meander loop and grid array antennas', *IEEE Trans. Antennas Propag.*, 2005, **53**, (10), pp. 3300–3307
11 Nakano, H., Kawano, T., Yamauchi, J.: 'Meander-line grid-array antenna', *IEE Proc. Microw. Antennas Propag.*, 1998, **145**, (4), pp. 309–312
12 Nakano, H., Osada, H., Yamauchi, J.: 'Strip-type grid array antenna with a two-layer rear-space structure'. Proc. 7th Int. Symp. Antennas Propag. & EM Theory, Guilin, China, October 2006, pp. 1–4
13 Xing, C., Kain, C., Kama, H.: 'A microstrip grid array antenna optimized by a parallel genetic algorithm', *Microw. Opt. Technol. Lett.*, 2008, **50**, (11), pp. 2976–2978
14 Chen, X., Wang, G., Huang, K.: 'A novel wideband and compact microstrip grid array antenna', *IEEE Trans. Antennas Propag.*, 2010, **58**, (2), pp. 596–599
15 Feng, P., Chen, X., Ren, X., Liu, C.-J., Huang, K.-M.:, 'A Novel Microstrip Grid Array Antenna with Both High-Gain and Wideband Properties', *Prog. In Electromagn. Res. C*, 2013, **34**, pp. 215–226
16 Wong, K.-L., Lin, Y.-F.: 'Microstrip-line-fed compact broadband circular microstrip antenna with chip-resistor loading', *Microw. Opt. Technol. Lett.*, 1998, **17**, (1), pp. 53–55
17 Harrington, R. F.: 'Effect of antenna size on gain, bandwidth, and efficiency', *J. Res. Nat. Bur. Stand.*, 1960, **64**, (1), pp. 1–12
18 Balanis, C. A.: 'Antenna theory: analysis and design', (John Wiley & Sons, 2012)